Journal of Experimental Botany, Vol. 70, No. 20 pp. 5971–5984, 2019
doi:10.1093/jxb/erz345 Advance Access Publication July 22, 2019
This paper is available online free of all access charges (see https://academic.oup.com/jxb/pages/openaccess for further details)

RESEARCH PAPER

Cell death regulation but not abscisic acid signaling is required for enhanced immunity to *Botrytis* in Arabidopsis cuticle-permeable mutants

Fuqiang Cui[1,2,*], Wenwu Wu[1], Kai Wang[2], Yuan Zhang[3], Zhubing Hu[4], Mikael Brosché[2,†], Shenkui Liu[1,*,†], and Kirk Overmyer[2,†]

[1] State Key Laboratory of Subtropical Silviculture, Zhejiang A&F University, Lin'an 311300, Hangzhou, China
[2] Organismal and Evolutionary Biology Research Program, Faculty of Biological and Environmental Sciences, and Viikki Plant Science Centre, University of Helsinki, PO. Box 65 (Viikinkaari 1), FI-00014 Helsinki, Finland
[3] Library of Donghu Campus, Zhejiang A&F University, Lin'an 311300, Hangzhou, China
[4] State Key Laboratory of Cotton Biology, Department of Biology, Institute of Plant Stress Biology, Henan University, Kaifeng, China

[†] These authors contributed equally to this study.
* Correspondence: fuqiang.cui@gmail.com or shenkuiliu@nefu.edu.cn

Received 2 April 2019; Editorial decision 15 July 2019; Accepted 16 July 2019

Editor: Robert Hancock, The James Hutton Institute, UK

Abstract

Prevailing evidence indicates that abscisic acid (ABA) negatively influences immunity to the fungal pathogen *Botrytis cinerea* in most but not all cases. ABA is required for cuticle biosynthesis, and cuticle permeability enhances immunity to *Botrytis* via unknown mechanisms. This complex web of responses obscures the role of ABA in *Botrytis* immunity. Here, we addressed the relationships between ABA sensitivity, cuticle permeability, and *Botrytis* immunity in the *Arabidopsis thaliana* ABA-hypersensitive mutants *protein phosphatase2c* quadruple mutant (*pp2c-q*) and *enhanced response to aba1* (*era1-2*). Neither *pp2c-q* nor *era1-2* exhibited phenotypes predicted by the known roles of ABA; conversely, *era1-2* had a permeable cuticle and was *Botrytis* resistant. We employed RNA-seq analysis in cuticle-permeable mutants of differing ABA sensitivities and identified a core set of constitutively activated genes involved in *Botrytis* immunity and susceptibility to biotrophs, independent of ABA signaling. Furthermore, *botrytis susceptible1* (*bos1*), a mutant with deregulated cell death and enhanced ABA sensitivity, suppressed the *Botrytis* immunity of cuticle permeable mutants, and this effect was linearly correlated with the extent of spread of wound-induced cell death in *bos1*. Overall, our data demonstrate that *Botrytis* immunity conferred by cuticle permeability can be genetically uncoupled from PP2C-regulated ABA sensitivity, but requires negative regulation of a parallel ABA-dependent cell-death pathway.

Keywords: BOS1, *Botrytis cinerea*, cell death, cuticle permeable, ERA1, farnesyl transferase, immunity, RNA sequencing.

Introduction

The necrotrophic fungal pathogen *Botrytis cinerea* is considered to be among the most important plant pathogens, both economically and as a model for research (Dean *et al.*, 2012). Multiple mechanisms determine the outcome of plant–*Botrytis* interactions, among which stress-hormone-regulated responses have been extensively studied (Mengiste, 2012; AbuQamar *et al.*, 2017). Jasmonic acid (JA) and ethylene signaling are essential and often function together in the activation of immunity to *Botrytis* (Mengiste, 2012), while salicylic acid (SA) signaling plays a lesser role (AbuQamar *et al.*, 2017). The

function of abscisic acid (ABA) signaling in defense against *Botrytis* is generally considered to be negative (Mengiste, 2012; AbuQamar *et al.*, 2017). Exogenous ABA application enhances *Botrytis* pathogenicity in a dose-dependent manner (Kettner and Dörffling, 1995; Shaul *et al.*, 1996; Audenaert *et al.*, 2002). Genetic evidence for the role of ABA is primarily based on loss-of-function (ABA-deficient or -insensitive) mutants, which exhibit enhanced immunity to *Botrytis* (Audenaert *et al.*, 2002; Asselbergh *et al.*, 2007; L'Haridon *et al.*, 2011). However, the evidence is not entirely consistent. We previously tested the *Botrytis* sensitivity of the ABA hyperaccumulation double mutant *cyp707a1 cyp707a3* in Arabidopsis, which is deficient in ABA inactivation, and did not find significantly increased *Botrytis* susceptibility compared with wild type (Okamoto *et al.*, 2006; Liu *et al.*, 2010*c*; Cui *et al.*, 2016). Furthermore, a recent study reported that exogenous ABA, applied 24 hours prior to infection, could prime the plant defense response and increase *Botrytis* immunity (Liao *et al.*, 2016). The resolution of this apparent contradiction may lie in the complexity of ABA signaling pathways. ABA signaling branches into many divergent downstream responses, which may differentially participate in regulating immunity to *Botrytis*.

ABA is required for cuticle formation (Curvers *et al.*, 2010; Cui *et al.*, 2016). Plants with impaired ABA signaling pathways are cuticle permeable. These mutants include the ABA biosynthesis mutants *aba deficient2* (*aba2*) and *aba3*; the ABA receptor mutants *pyrabactin resistance1* (*pyr1*)/*pyr1-like* (*pyl*)/*regulatory components of aba receptors* (*rcar*); and the triple mutant of the three core kinases in ABA signaling, *snf1-related protein kinase* (*snrk*)*2.2 snrk2.3 snrk2.6* (here abbreviated to *snrk2.236*) (Curvers *et al.*, 2010; L'Haridon *et al.*, 2011; Cui *et al.*, 2016). These ABA mutants are also more resistant to *Botrytis* (L'Haridon *et al.*, 2011; Cui *et al.*, 2016). Although the cuticle acts as a barrier to exclude pathogens (Riederer, 2007), a defective cuticle confers strong immunity to *Botrytis* (Bessire *et al.*, 2007) that is independent of the canonical antifungal defense signaling pathways, JA, ethylene, SA, and camalexin (Chassot *et al.*, 2007; Serrano *et al.*, 2014). Although the mechanism for this phenomenon remains unknown, it is thought that a permeable cuticle could facilitate early or enhanced perception of *Botrytis* (Asselbergh *et al.*, 2007; Ziv *et al.*, 2018). Other biological processes may also be involved, including defense activation by cuticle damage-associated molecular patterns, secretion of antifungal compounds, generation of reactive oxygen species (ROS), control of cell death, altered metabolism, and altered foliar microbiome composition (Kliebenstein *et al.*, 2005; Asselbergh *et al.*, 2007; Bessire *et al.*, 2007; Chassot *et al.*, 2007; Curvers *et al.*, 2010; L'Haridon *et al.*, 2011; Seifi *et al.*, 2013; Ritpitakphong *et al.*, 2016). Thus, this strong enhanced *Botrytis* immunity may be multilayered, involving several of the processes listed above. Remarkably, no genetic suppressors of this phenotype have been reported.

ABA is also an important regulator of abiotic stresses and cell death. Treating plants with ABA leads to leaf chlorosis and cell death (Fan *et al.*, 1997; Jiang and Zhang, 2001; Takasaki *et al.*, 2015; Zhao *et al.*, 2016). Thus, it is possible that high levels of ABA trigger cell death to promote plant susceptibility to *Botrytis*. Indeed, mutants with enhanced cell death after ABA treatment were reported to be susceptible to *Botrytis*. *BOTRYTIS SUSCEPTIBLE1* (*BOS1*) is a MYB-type transcription factor (MYB108; Mengiste *et al.*, 2003). The *bos1* mutant exhibits enhanced cell-death spread in an ABA-dependent manner (Cui *et al.*, 2013). Accordingly, *bos1* is hypersensitive to *Botrytis* (Mengiste *et al.*, 2003). *HOOKLESS1* (*HLS1*) encodes a putative histone acetyltransferase, and the *hls1* mutant exhibits increased cell death upon ABA application and enhanced susceptibility to *Botrytis* (Liao *et al.*, 2016). Interestingly, a germination assay showed that *hls1* is ABA insensitive (Liao *et al.*, 2016). Thus, testing different mutants with altered ABA sensitivities would help to clarify the relationship between ABA sensitivity and cell death control in plant–*Botrytis* interactions.

To further address these issues, we examined two additional ABA-hypersensitive mutants, *enhanced response to aba1* (*era1*) and the *PROTEIN PHOSPHATASE TYPE 2C* (*PP2C*) quadruple knockout mutant, *aba insensitive1*-2 (*abi1*-2) *abi2*-2 *hypersensitive to aba1-1* (*hab1-1*) *pp2ca-1* (Rubio *et al.*, 2009) (here abbreviated to *pp2c-q*). *ERA1* encodes the beta subunit of farnesyl-trans-transferase; this enzyme transfers farnesyl groups to target proteins at the consensus sequence CaaX (Galichet and Gruissem, 2003). Only two confirmed ERA1 substrates are known, ALTERED SEED GERMINATION2 (ASG2) and the cytochrome P450 CYP85A2. Loss of function in these loci results in alterations in different aspects of ABA signaling (Dutilleul *et al.*, 2016; Northey *et al.*, 2016). Predicted targets potentially subject to ERA-dependent farnesylation include 700 proteins in Arabidopsis (Northey *et al.*, 2016). Accordingly, the *era1* mutant is pleiotropic, with altered responses in multiple biological processes, including enhanced ABA sensitivity, late flowering, enlarged organs, and increased susceptibility to *Hyaloperonospora parasitica* and *Pseudomonas syringae* pv. *maculicola* (Cutler *et al.*, 1996; Pei *et al.*, 1998; Galichet and Gruissem, 2003, 2006; Goritschnig *et al.*, 2008). Whether farnesyl-trans-transferase is involved in cuticle formation has not been reported. *PP2Cs* directly interact with the PYR/PYL ABA receptors and negatively regulate ABA signaling (Park *et al.*, 2009). Hence, the *pp2c-q* mutant exhibits constitutively activated ABA signaling (Antoni et al., 2013). Using these two ABA-hypersensitive mutants, we dissected the relationships between ABA sensitivity, cuticle permeability, cell death, and sensitivity to *Botrytis*.

Materials and methods

Growth conditions and plant material

Seeds were germinated at high density on a mixture of peat and vermiculite (2:1) after stratification at 4 °C for 2 days. One-week-old seedlings were transplanted, two per pot, in the same soil mixture. Plants were grown in a growth chamber with conditions of 150–200 μmol m^{-2} s^{-2} light intensity, 12/12 h (light/dark) photoperiod, 60% humidity, and 23/18 °C (day/night) temperature. For double mutant construction, *lacs2.3* and *bos1* were used as pollen donors to pollinate *era1-2*. In the F_2 generation, seedlings with *era1* phenotypes were genotyped with primers of each of the other genotypes. To circumvent the sterility of the *bos1 era1-2* double mutant, segregating populations of F_2 plants were phenotyped and genotyped to identify plants for use in experiments. The *era1*-like plants were selected for experiments and then genotyped with *bos1* primers. Only the data of true *bos1 era1-2* double mutants were recorded.

ABA-related mutants used in this study were *aba3* (*aba deficient3*); *abi1-1* (*aba insensitive1*); *snrk2.236* (*snf1-related protein kinase2.2 snrk2.3 snrk2.6*

triple mutant); *pp2c-q* (*protein phosphatase2c* quadruple mutant *abi1-2 abi2-2 hab1-1 pp2ca-1*); *era1* (*enhanced response to aba1*); and *112458* [sextuple mutant of *pyrabactin resistance1* (*pyr1*) *pyr1-like1* (*pyl1*) *pyl2 pyl4 pyl5 pyl8*]. Putative ERA1 target mutants were *cyp85a2*, *asg2-1*, and *asg2-2*, and are described in Jalakas *et al.* (2017).

Arabidopsis thaliana Columbia (Col-0) was used in all experiments. All mutant alleles used were confirmed by PCR genotyping. Mutants were obtained from the European Arabidopsis Stock Centre (http://arabidopsis.info/) or were gifts (see Acknowledgements).

Fungal cultivation and disease assays

Botrytis cinerea strain BO5.10 was grown on potato dextrose agar. For conidia production, spores with mycelium were collected using forceps into 1/3 strength potato dextrose broth, mixed, filtered, and diluted to 2×10^6 spores ml^{-1}. For lesion size assays, 3 µl drops were inoculated on to leaves of 24-day-old plants, closed in a moist tray at 100% humidity, and transferred to a growth chamber with conditions of 180 µmol m^{-2} s^{-2}, 12/12 h light/day at 21 °C. Lesions were photographed at 3 days post infection (dpi) and their diameters were measured by using ImageJ (http://rsb.info.nih.gov/ij/). Spray infections were done using conidia suspension as described above with sprayers on the whole rosettes of 24-day-old plants.

Tissue staining and wounding assays

Dye exclusion experiments were performed with fully expanded leaves from 24-day-old plants, for 20 min with immersion treatment or for 2 h with 5 µl droplets of a 0.05% solution of toluidine blue stain as described by Tanaka *et al.* (2004). The stained areas were measured with ImageJ according to Cui *et al.* (2016). Wounding-induced cell death was determined from leaves punctured with a needle. Wounded leaves at 6 days post wounding (dpw) were subjected to trypan blue staining to visualize the cell death. Samples were photographed with a stereomicroscope (Olympus SZX16, Japan) and measured with ImageJ. Each lesion was measured four times through its center. The mean of the four lengths of each wound was taken as the length of spread of cell death. For assessment of H_2O_2 production and *Botrytis*-induced cell death, spray-infected rosette leaves were stained with 3,3′-diaminobenzidine (DAB; D8001, Sigma-Aldrich) at 16 hours post infection (hpi) and trypan blue (T6146, Sigma) at 36 hpi. The stained leaves were mounted in water to eliminate reflection before being photographed with a stereomicroscope (Olympus SZX16, Japan). The DAB- and trypan blue-stained area and whole leaf area in each sample were measured with ImageJ. The percentage stained area was calculated by dividing the stained area by the whole leaf area.

RNA-seq and data analysis

Botrytis-infected and mock-sprayed plants (five rosettes of each genotype) were collected at 20 and 44 hpi. Three biological replicates were used. All samples were collected at 15.00 h to eliminate the influence of circadian-regulated genes. RNA was extracted with the MiniBEST Universal RNA Extraction Kit (TaKaRa). The total RNA of each sample ranged from 13.8 to 41 µg, with an RNA quality score (RQS) value from 6.7 to 8.5. The RNA-seq was executed by using an Illumina HiSeq 4000 in 150 bp paired-end sequencing. By filtering out adaptors and low-quality reads using Trimmomatic-0.38 (Bolger *et al.*, 2014), we obtained at least 8 Gb clean reads for each sample. The clean data have been uploaded to the NCBI Sequence Read Archive (https://www.ncbi.nlm.nih.gov/sra, accession number PRJNA495475). The clean reads were then aligned to the reference *A. thaliana* genome (release: TAIR10.v32 download from Ensembl Plants) using hisat2 v2.1.0 (Kim *et al.*, 2015) with a modification of intron length for plants (--min-intronlen 20 --max-intronlen 5000). StringTie v1.3.4d (Pertea *et al.*, 2015) was used to construct the new transcripts and generate the merged gene annotations. Finally, to obtain a high confidence of differentially expressed genes (DEGs), at least two of three programs, cuffdiff (Trapnell *et al.*, 2013), edgeR (Robinson *et al.*, 2010), and DESeq2 (Love *et al.*, 2014), were used to determine the DEGs with $P\leq0.05$ and absolute ($\log_2$ fold change) ≥ 1. DEGs were used to create Venn diagrams using Venny 2.1 (https://bioinfogp.cnb.csic.es/tools/venny). Gene Ontology (GO) enrichment was analyzed with the online tools of the Gene Ontology Consortium (http://geneontology.org/page/go-enrichment-analysis) and then the exported data were used to render the GO enrichment pictures in R. For heatmap construction, the heatmap2 package in R was used and then manually adjusted with CorelDRAW (X4) software.

qPCR assay

For confirming gene expression of the RNA-seq data, RNA isolation was performed with the same plant material used for RNA-seq and then treated with DNase I. Real-time quantitative PCR (qPCR) was performed as described by Cui *et al.* (2016) using *YLS8* (AT5G08290), *TIP41* (AT4G34270), and *PP2AA3* (AT1G13320) as reference genes. Primer sequences are given in Supplementary Table S6 at *JXB* online. For *Botrytis* growth assays, fungal DNA was extracted from 10 leaf discs (7 mm diameter) from infected plants and qPCR was performed according to Gachon and Saindrenan (2004), using specific primers for cutinase A. The raw cycle threshold values were analyzed with Qbase (Hellemans *et al.*, 2007).

Statistical analysis

Statistical analysis of lesion sizes and cell death spread were carried out with scripts in R (version 3.0.3). Using the nlme package, a linear mixed model with fixed effects for genotype, treatment, and their interaction was fitted to the data, plus a random effect for biological repeat. The model contrasts were estimated with the multcomp package, and the estimated *P*-values were subjected to single-step *P*-value correction. A logarithm of the data was taken before modeling to improve the model fit. The qPCR data were $\log_{10}$-transformed and significance was estimated with a two-tailed Student's *t*-test using equal variance. The significance of overlaps between two gene sets was evaluated with Fisher's exact test in R.

Results

Enhanced immunity to Botrytis *in* era1-2

Botrytis infections of two ABA-hypersensitive mutants, *enhanced response to aba1-2* (*era1-2*) and *pp2c-quadruple* (*pp2c-q*), revealed phenotypes inconsistent with the enhanced susceptibility that would be predicted based on the assumption that ABA acts solely as a negative regulator of *Botrytis* immunity (Fig. 1A). Disease progression in *era1-2* was reduced, measured as smaller lesion size (Fig. 1B) and less *Botrytis* DNA accumulation (measured with real-time qPCR; Fig. 1C). The extent of cell death was also reduced in *era1-2* (Fig. 1D, F). The *Botrytis* immunity associated with two additional *era1* alleles, *era1-7* and *era1-8*, was also enhanced compared with the wild type (Supplementary Fig. S1).

To identify potential mechanisms of enhanced immunity in *era1-2*, we monitored ROS accumulation during *Botrytis* infection. Strong H_2O_2 accumulation in *Botrytis*-infected *era1-2* was documented via DAB staining at 16 hpi (Fig. 1E, G). This suggests that the enhanced immunity phenotype of *era1-2* may be due to early and/or enhanced ROS production.

ERA1 and cuticle development

An early *Botrytis*-induced H_2O_2 burst is associated with cuticle permeability (Asselbergh *et al.*, 2007; L'Haridon *et al.*, 2011), prompting us to assay for this phenotype. Toluidine blue staining is a classical cuticle-permeability assay: cuticle-defective leaves fail to exclude the dye, resulting in dark blue staining (O'Brien *et al.*, 1964; Tanaka *et al.*, 2004). The *era1-2* mutant stained dark blue, while the wild type and *pp2c-q* did not (Fig.

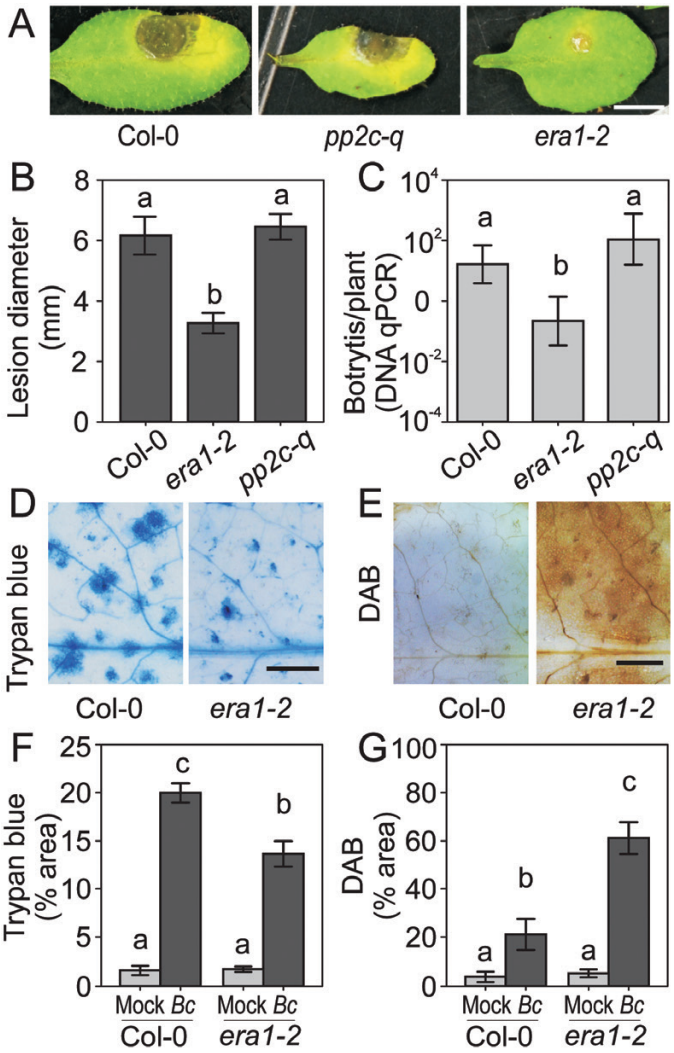

Fig. 1. Enhanced *Botrytis* immunity in the ABA hypersensitive *era1-2* mutant. (A) *Botrytis* infection of Col-0, *pp2c-quad*, and *era1-2*. Droplets of *Botrytis* conidia suspensions (3 µl, 2×10^6 spores ml^{-1}) were applied to 24-day-old fully expanded leaves. Photographs were taken at 3 days post infection (dpi). Scale bar=5 mm. (B) Quantitative data of lesion sizes in (A). The lesion diameters were measured with ImageJ. Combined results of four experiments (n=10 in each independent biological repeat) were analyzed in a linear mixed model with single-step P-value adjustment. Error bars represent the SE of means. Different letters above the bars indicate significant differences (P<0.05). (C) DNA of *Botrytis* on leaves at 3 dpi was quantified with real-time qPCR using the Arabidopsis actin gene as a control. Different letters indicate significant differences (two-tailed t-test, P<0.05). (D–G) Leaves were stained at 36 hours post infection (hpi) for cell death with trypan blue (D, F), and at 16 hpi for H_2O_2 accumulation with 3,3′-diaminobenzidine (E, G). The percentage stained area was used for comparisons between Col-0 and *era1-2*. Two biological repeats with seven leaves in each repeat were analyzed with a linear model. Different letters above the bars indicate significant differences (P<0.05). Scale bar=2 mm.

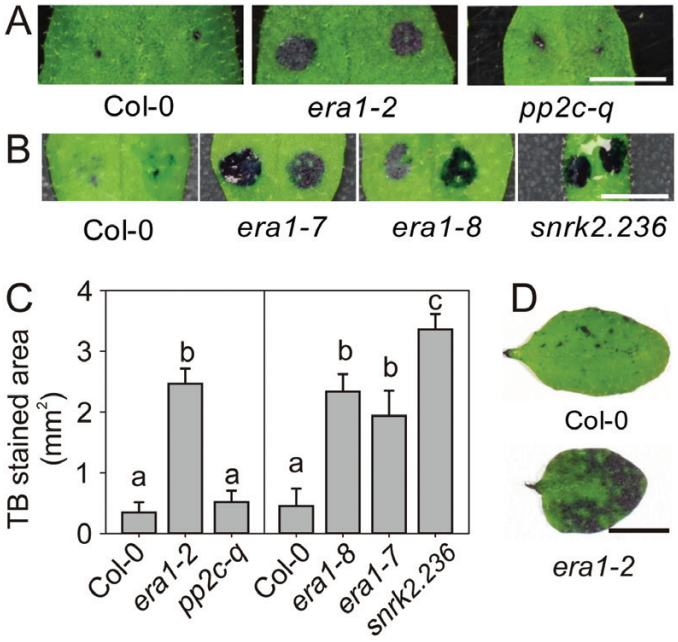

Fig. 2. Enhanced cuticle permeability in the ABA hypersensitive *era1-2* mutant. (A, B) The cuticle of *era1-2* was more permeable than other mutants or the wild type Col-0 under toluidine blue staining. Leaves of 24-day-old plants were stained with 5 µl droplets of 0.05% toluidine blue solution for 2 h. The ABA-insensitive *snrk2.236* was used as a positive control. (C) Quantification of the toluidine blue-stained areas. Combined results of three experiments (n=12 in each independent biological repeat) were analyzed in a linear mixed model with single-step P-value adjustment. Error bars represent the SE of means. Different letters above the bars indicate significant differences (P<0.05). (D) Leaves immersed in toluidine blue solution for 20 min. Bar=5 mm.

2A). To exclude the possibility of second site mutations independent of *era1*, we confirmed enhanced permeability in mutants in two additional alleles, *era1-7* and *era1-8* (Goritschnig *et al.*, 2008), using the ABA-insensitive *snrk2.236* as a positive control (Fig. 2B, C). The enhanced permeability of the *era1-2* mutant was further tested with an immersive staining assay, in which the *era1-2* leaf stained mostly dark while the wild-type leaf remained unstained (Fig. 2D). Knockout mutants of ASG2 and CYP85A2, the two known ERA1 substrates that are involved in modulating the ABA response, exhibited normal cuticle permeability (Supplementary Fig. S2), suggesting that the role of ERA1 in cuticle formation is independent of these loci.

Overall, our findings genetically uncoupled ABA sensitivity from *Botrytis* susceptibility and revealed that *ERA1* is required for cuticle formation and negatively regulates *Botrytis* immunity.

ABA-independent genes deregulated in cuticle-defective mutants

As *era1-2* displayed *Botrytis* immunity, enhanced ABA sensitivity, and a permeable cuticle (Figs 1 and 2), it was utilized as a tool to further explore the relationships between these phenotypes. We used *era1-2*, *snrk2.236*, and the cuticle biosynthesis mutant *lacs2.3* (Bessire *et al.*, 2007; Tang *et al.*, 2007), to examine global transcriptional changes under *Botrytis* infection and control conditions. All three mutants are cuticle permeable and *Botrytis* resistant, whereas their ABA sensitivities are largely different: *era1-2* is hypersensitive, *lacs2.3* is moderately sensitive, and *snrk2.236* is strongly insensitive (Bessire *et al.*, 2007; Fujii and Zhu, 2009; Cui *et al.*, 2016). These three mutants allowed us to identify the effects of ABA sensitivity and reveal the core genes involved in the enhanced *Botrytis* immunity conditioned by cuticle deficiency.

Mock-treated and *Botrytis* spore-suspension-infected plants were sampled at 20 hpi. To control for genes under circadian regulation, the second time point was 24 hours later (44 hpi).

Samples of three biological repeats were subjected to RNA-seq analysis. To identify the core genes potentially involved in immunity to *Botrytis* in cuticle-defective mutants (CDMs), we first defined the significantly up-/down-regulated genes in each of the CDMs compared with the wild type. The genes that were mis-regulated in each CDM with fold change ≥2 and $P \leq 0.05$ in comparison to the wild type were chosen for further analysis (Supplementary Table S1). The mock-treated CDMs shared a common set of 64 genes with increased expression and seven with decreased expression (Fig. 3A; Supplementary Table S2A, B). Additionally, each mutant had its own unique set of DEGs, but generally *lacs2* and *snrk2.236* were more similar to each other than to *era1-2* (Fig. 3A). Under *Botrytis* treatment, the three CDMs had in common 53 genes with increased expression and 25 genes with decreased expression (Fig. 3B; Supplementary Table S2C, D). As in the mock-treated condition, each single mutant had its own unique set of mis-regulated genes (Fig. 3B). Further analysis focused on the genes that were commonly regulated in all three CDMs, as these could be considered as ABA-independent genes and

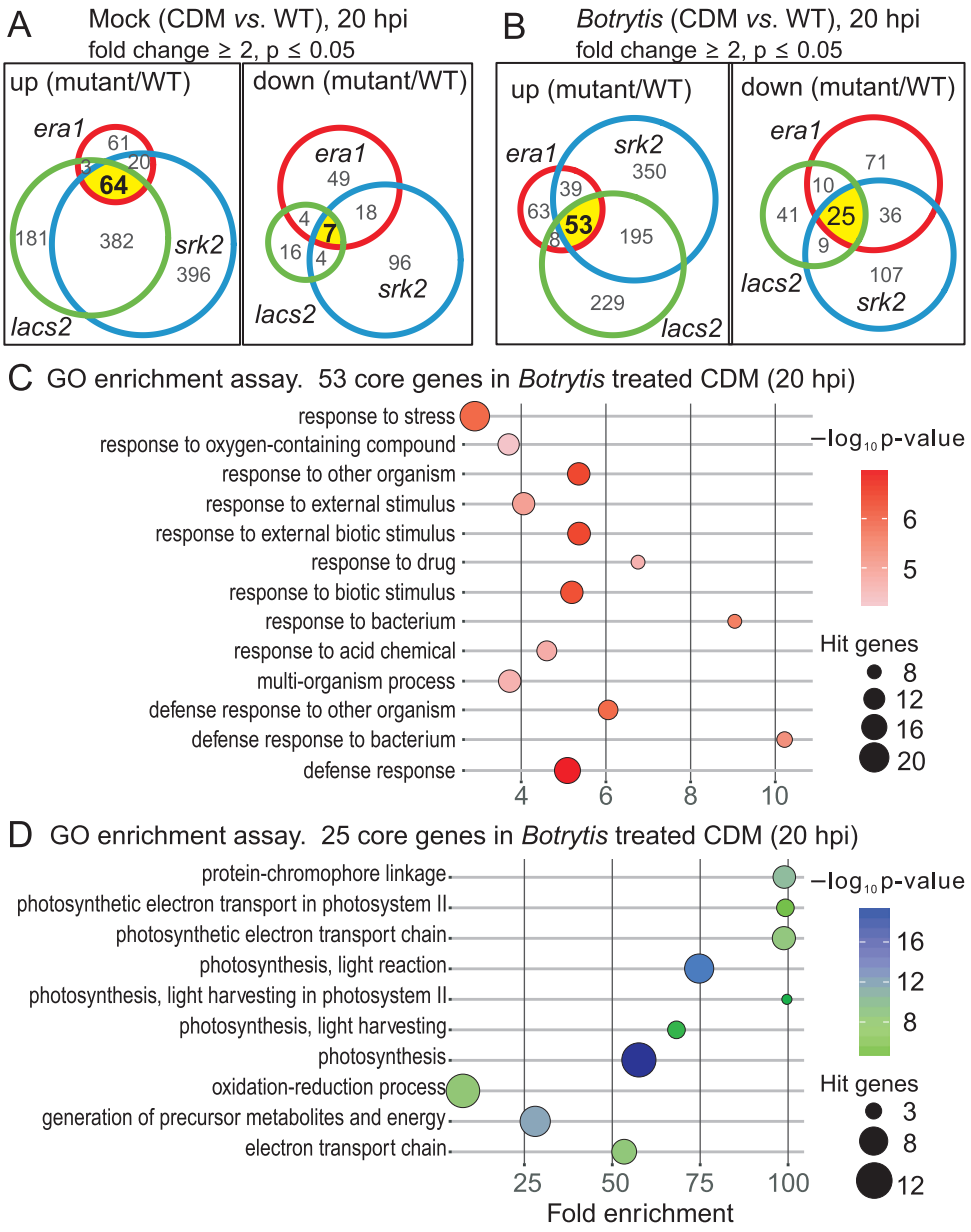

Fig. 3. Analysis of the differentially expressed genes (DEGs) in cuticle-defective mutants (CDMs) compared with Col-0 in mock and *Botrytis* treatments. Plants at 24 days old were sprayed with 2×10^6 ml^{-1} *Botrytis* spores. Samples were collected at 20 and 44 hours post infection (hpi) for RNA-seq analysis. (A) DEGs in the CDMs under mock treatment. DEGs were identified in comparison between each CDM and wild type (fold change ≥2 and $P \leq 0.05$; see also Supplementary Table S2). There were 64 genes commonly up-regulated (left) and seven genes down-regulated (right) in the CDMs (genes are listed in Supplementary Table S2A, B). Mutant names are abbreviated: *era1-2* to *era1*, *lacs2.3* to *lacs2*, *snrk2.236* to *srk2*. (B) DEGs under *Botrytis* treatment in the CDMs. There were 53 genes commonly up-regulated (left) and 25 genes down-regulated (right) in the CDMs (genes are listed in Supplementary Table S2C, D). The DEGs at 44 hpi are presented in Supplementary Fig. S3B and Supplementary Table S2E, F. (C, D) GO enrichment analysis of the core genes in (B). The 53 up-regulated genes were enriched in defense-related terms (C). The 25 down-regulated genes were enriched exclusively in photosynthesis-related terms (D). The GO enrichment analysis of the core genes of mock-treated CDMs at 20 hpi is presented in Supplementary Fig. S3A.

may function as CDM-specific components that regulate plant immune responses to *Botrytis*.

In mock-treated CDMs, multiple receptor-like kinase genes related to defense responses and wounding-responsive genes were up-regulated. (Supplementary Table S2A). In addition, genes required for the pathogenicity of biotrophic or hemibiotrophic pathogens or with negative roles in SA-regulated defense responses were up-regulated (Supplementary Table S2A). For selected genes, RNA-seq data were confirmed with real-time qPCR (Supplementary Fig. S4).

In the *Botrytis*-treated CDMs, the core up-regulated genes were quite similar to the mock-treated CDMs, as seen in the GO enrichment analysis (Fig. 3C; Supplementary Fig. S3A). The term 'defense response to bacterium' was enriched (Fig. 3C). A common set of genes was up-regulated in the mock-treated CDMs and *Botrytis*-treated CDMs; these included *Cysteine-rich receptor-like protein kinase* (*CRK*) family and other kinase genes, salicylic acid signaling genes, and other pathogen-defense-related genes, including the metacaspase gene *MC2* (Supplementary Table S2C; Supplementary Fig. S4).

There were also genes specifically up-regulated only in the *Botrytis*-treated CDMs (Supplementary Table S2C; Supplementary Fig. S4); these included *Enhanced Disease Resistance4* and *Downy Mildew Resistant6*, two SA-regulated genes that are required for plant susceptibility to the biotrophic powdery mildew pathogen (van Damme *et al.*, 2008; Wu *et al.*, 2015). Only a few genes possibly related to *Botrytis* immunity were up-regulated in the *Botrytis*-treated CDMs, such as the P450 family member *CYP82C2*, which is required for the activation of JA signaling and the synthesis of a cyanogenic metabolite to defend against *Botrytis* (Liu *et al.*, 2010*a*; Rajniak *et al.*, 2015). In the *Botrytis*-treated CDMs, 25 genes were identified as the core down-regulated genes (Fig. 3B). Most of these genes are related to functions in the chloroplast and photosynthesis (Fig. 3D; Supplementary Table S2D).

Overall, the core genes mis-regulated in CDMs were mainly genes previously implicated in pathogen defense responses or SA signaling. This finding indicated that a signal derived from the defective cuticle may lead to the activation of defense responses, ultimately resulting in *Botrytis* immunity.

ABA signaling in the transcriptional response to Botrytis

We further compared the *Botrytis*-regulated genes at 20 and 44 hpi between the wild type and CDMs. DEGs were identified in each genotype and were compared between genotypes (Fig. 4). At 44 hpi, substantially fewer DEGs were observed in all three CDMs compared with the wild type. This was likely due to the strong immunity in these mutants; that is, there was less dead tissue in the mutants compared with the wild type (Fig. 1; Bessire *et al.*, 2007; Cui *et al.*, 2016).

Col-0 had the most *Botrytis*-regulated genes, followed by *era1-2*, *lasc2.3*, and then *snrk2.236* (Fig. 4). The number of *Botrytis*-regulated genes in the mutants correlated with their ABA sensitivity. This indicated that in the CDMs, the extent of ABA sensitivity still influenced transcriptional responses to *Botrytis*. To

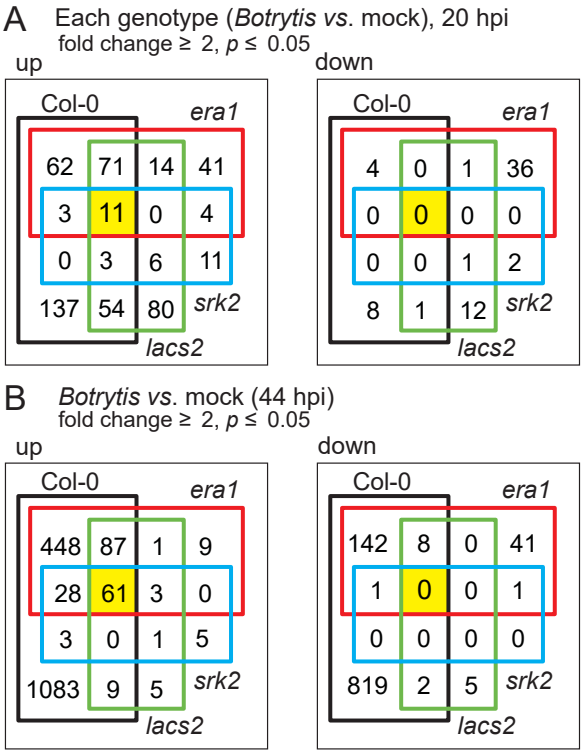

Fig. 4. Identification of *Botrytis*-induced differentially expressed genes (DEGs). DEGs were identified in comparisons between *Botrytis*-treated CDMs and Col-0 to their corresponding genotype under mock treatment (fold change ≥2 and $P \leq 0.05$; see also Supplementary Table S3). (A) At 20 h post infection (hpi), there were 11 genes commonly up-regulated (left) and no common genes down-regulated (right) in the *Botrytis*-treated genotypes. The genes are listed in Supplementary Table S3E. Mutant names are abbreviated: *era1-2* to *era1*, *lacs2.3* to *lacs2*, *snrk2.236* to *srk2*. (B) At 44 hpi, there were 61 genes commonly up-regulated (left) and no common genes down-regulated (right) in the *Botrytis* treated genotypes. The genes are listed in Supplementary Table S3J.

further explore the relation between ABA and *Botrytis* in transcriptional regulation, we made a comparison between *Botrytis*-regulated and ABA-regulated genes (Supplementary Fig. S5; Supplementary Table S4) using publicly available data from an ABA RNA-seq experiment (50 μM ABA, 3h; Zhu *et al.*, 2017). Significant overlap was observed between up-regulated genes at both 20 and 44 hpi, and for down-regulated genes at 44 hpi (Supplementary Fig. S5A). The genes commonly regulated by both ABA and *Botrytis* were subjected to a GO enrichment analysis (Supplementary Table S4; Supplementary Fig. S6). The GO terms 'toxin catabolic process', 'glutathione metabolic process', 'response to oxidative stress', and 'response to hydrogen peroxide' were enriched in the overlap of ABA- and *Botrytis*-induced genes (Supplementary Fig. S6A, B). Genes down-regulated by ABA and *Botrytis* at 44 hpi were enriched for 'syncytium formation' and 'plant-type cell wall loosening and modification' (Supplementary Fig. S6C). Taken together, these data indicate that exogenous ABA likely activates signaling required for a subset of plant responses to *Botrytis*.

Expression of previously identified Botrytis*-response genes*

Extensive research on the interactions between *Botrytis* and Arabidopsis has identified several positive and negative regulators. We constructed a list of these genes through keyword searches of TAIR (https://www.arabidopsis.org; Supplementary Table S5). The genes related to the JA, ethylene, and PAD3 pathways were excluded, as the *Botrytis* immunity mediated by cuticle permeability was previously shown to be independent of these signaling pathways (Chassot *et al.*, 2007). Expression values (log_2 of the number of transcripts per million) for each gene were used to build a heatmap (Fig. 5). The expression of most genes was similar among genotypes and treatments (Fig. 5), indicating that these genes were not *Botrytis* inducible or cuticle dependent. However, the expression of some genes, including the autophagy inducer *BAG6* (Li *et al.*, 2016), the cell-death regulator *BOS1* (Mengiste *et al.*, 2003; Cui *et al.*, 2013), and several pectin methylesterase inhibitors (*PMEIs*; Lionetti *et al.*, 2017), had increased expression at 44 hpi (Fig. 5). The expression of these genes was genotype dependent; the wild type showed the highest expression, *era1-2* showed moderate expression, while *snrk2.236* and *lacs2.3* showed the lowest expression (Fig. 5). We propose that the expression of these genes may be correlated to cell-death control and lesion development, as *Botrytis* extracts nutrients from dead and dying tissue. Hence, less expression of these genes would be seen in highly *Botrytis*-tolerant genotypes. Furthermore, cell-death control is a key factor that determines lesion development in cuticle-defective plants (Asselbergh *et al.*, 2007; Curvers *et al.*, 2010; Seifi *et al.*, 2013). Thus, we chose the *bos1* mutant, which exhibited mis-regulated cell-death development (Cui *et al.*, 2013), for further analysis in relation to the other mutants used in this study.

The enhanced Botrytis *immunity of* era1-2 *is BOS1 dependent*

We constructed the *bos1 era1-2* double mutant to test whether the BOS1-regulated control of cell death was required for the

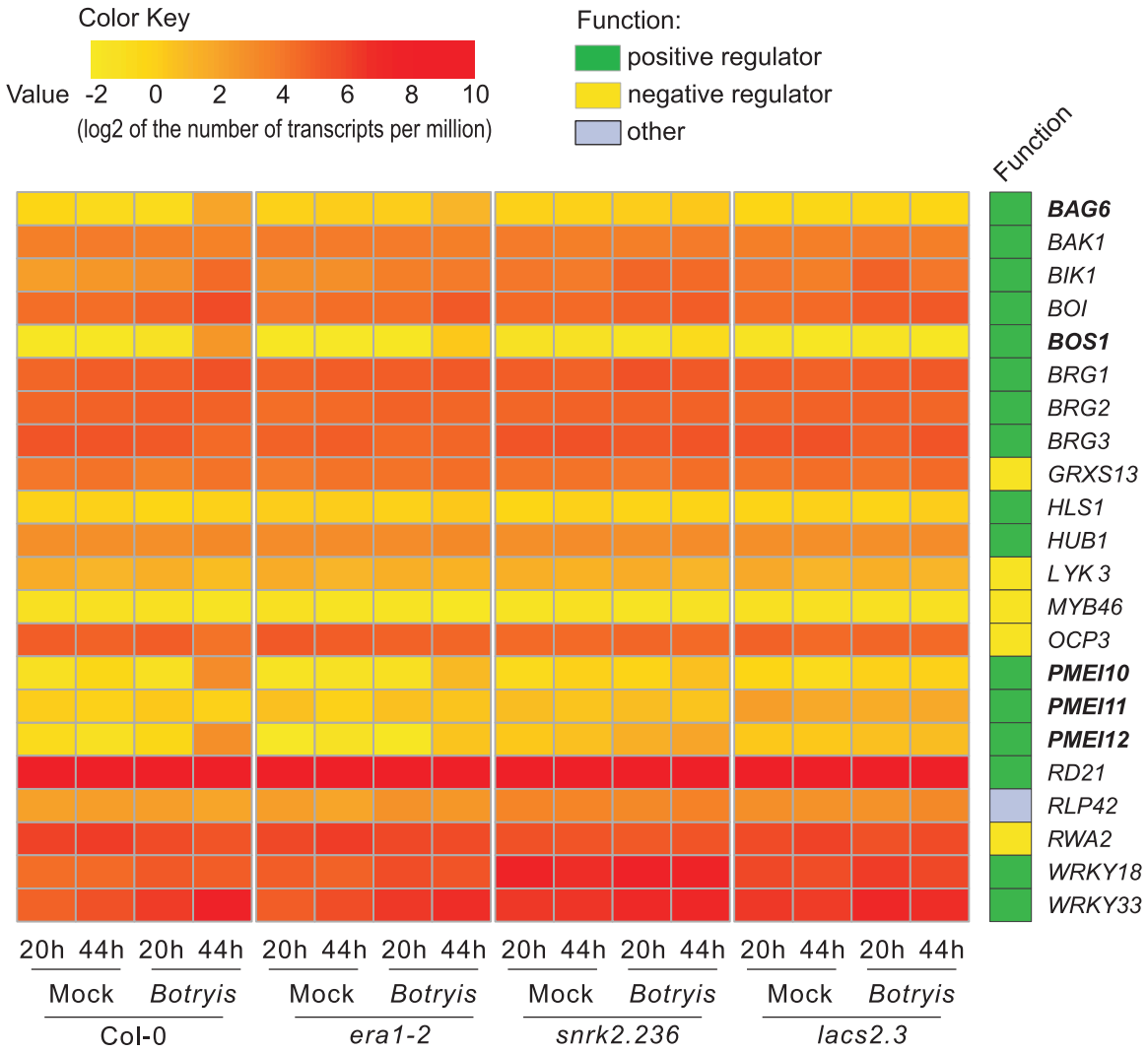

Fig. 5. Relative expression of genes known to regulate *Botrytis* immunity. The gene list was obtained from https://www.arabidopsis.org via the gene searching tool with the keywords '*Botrytis*' or '*B. cinerea*'. Genes related to the jasmonic acid, ethylene, and PAD3 pathways were excluded, as they are not required for *Botrytis* immunity conferred by cuticle permeability (Chassot *et al.*, 2007). The expression values (log_2 of the number of transcripts per million) for each gene were used to build a heatmap. The genes are listed in alphabetical order. The treatments were mock and *Botrytis* spray infection at the indicated time points and are grouped according to genotypes.

immunity to *Botrytis* associated with cuticle-defective plants. Interestingly, the enhanced immunity of *era1-2* was fully suppressed in *bos1 era1-2* (Fig 6A, B). The lesion sizes of *Botrytis*-infected *bos1 era1-2* leaves were markedly larger than those of *era1-2* (Fig. 6A) and were very similar to those of the *bos1* single mutant (Fig. 6B). We previously demonstrated that *bos1* exhibited uncontrolled runaway cell death after wounding (Cui *et al.*, 2013). Thus, we assessed cell death initiated from needle-puncture wounds in *bos1*, *era1-2*, and the *bos1 era1-2* double mutant. Dead tissue was visualized by trypan blue staining and quantified by measuring the length from the wound edge to the frontier of the spreading dead tissue (Fig. 6C). We found that the spread of cell death in *bos1 era1-2* was slightly but not significantly greater than in *bos1* (Fig. 6C, D). This indicated that the cell-death control conferred by BOS1 is required for the *Botrytis* immunity of the *era1-2* mutant.

Compared with *bos1*, cell death in *bos1 era1-2* was developmentally enhanced in older plants, as *bos1 era1-2* exhibited spontaneous cell death during flowering (Fig. 6E). We observed that once buds started opening, cell death initiated in the buds and then spread along the shoots (Fig. 6E); this led to a sterility phenotype, with no *bos1 era1-2* seeds obtained.

To test whether loss of BOS1 function could suppress the enhanced *Botrytis* immunity of other CDMs, we made the *bos1 lacs2.3* double mutant. The *bos1* mutation restored the *Botrytis* susceptibility of *lacs2.3* to wild-type levels (Fig. 7A, B). Furthermore, runaway cell death in *bos1 lacs2.3* was more extensive than in the wild type, but significantly less extensive than in the *bos1* single mutant (Fig. 7C, D). The early ROS burst present in cuticle-permeable mutants under *Botrytis* treatment was assessed in *bos1 era1-2* and *bos1 lacs2.3*, but was unaltered in both double mutants compared with the respective *era1-2* and *lacs2.3* single mutants (Supplementary Fig. S7). Taken together, these findings indicate that cell-death control is required, but

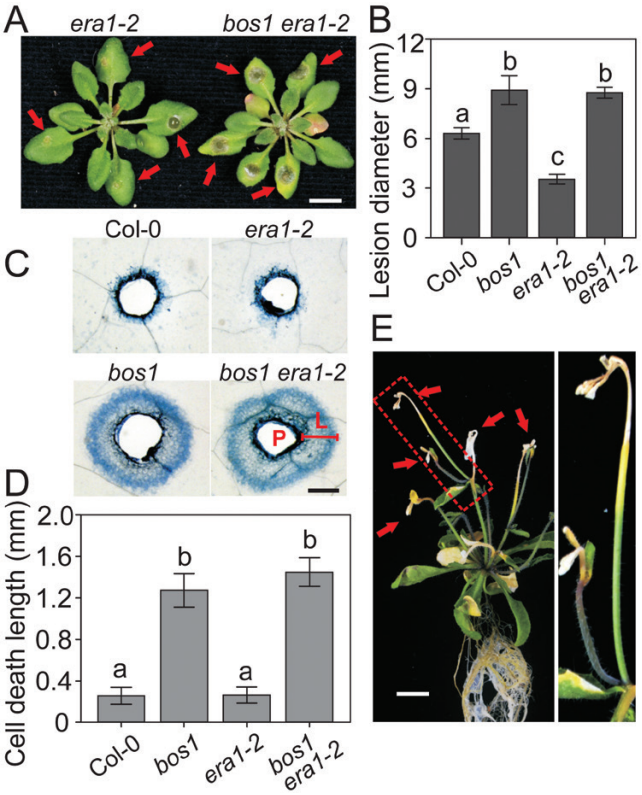

Fig. 6. The *Botrytis* immunity of *era1-2* was fully suppressed by *bos1*. (A) Typical lesion symptoms of *era1-2* and *bos1 era1-2*. The arrows indicate *Botrytis*-infected lesions. Droplets of *Botrytis* conidia suspensions (3 μl, 2×10^6 spores ml^{-1}) were applied to 24-day-old fully expanded leaves. Photographs were taken at 3 dpi. Scale bar=1 cm. (B) Quantitative lesion size data. The lesion diameters were measured with ImageJ. Combined results of three biological experiments (n=36 in total) were analyzed in a linear mixed model with single-step P-value adjustment. Error bars represent the SE of means. Different letters above the bars indicate significant differences (P<0.05). (C) Representative wound-induced cell death symptoms stained with trypan blue. Needle-punctured leaves were stained with trypan blue at 6 days post wounding to detect cell death. L, Length of cell death spread; P, puncture site. Scale bar=1 mm. (B) Quantitative spreading cell death data. The length of spread of cell death was measured as indicated in (C) around each wound four times in four directions (up, down, left, and right), and the mean value was used. Data of three repeats were analyzed in a linear mixed model with single-step P-value adjustment. Error bars represent the SE of means. Different letters above the bars indicate significant differences (P<0.05). (E) Spreading cell-death symptoms were enhanced in *bos1 era1-2*. Four-week-old *in vitro*-grown plants are shown. Once buds started opening, cell death initiated in the buds and then spread along the shoots, eventually causing the death of the whole plant. Right panel, close-up of the area indicated by the dashed box in the left panel. Arrows indicate dead buds. Scale bar=1 cm.

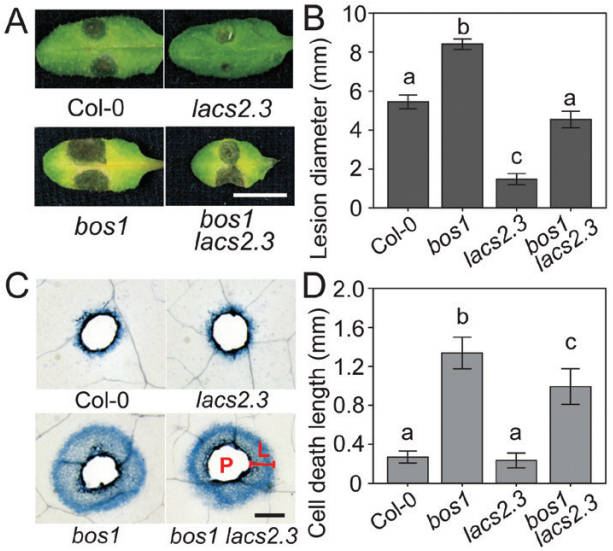

Fig. 7. *Botrytis* immunity in *lacs2.3* was attenuated in the *bos1 lacs2.3* double mutant. (A) Typical lesion symptoms of *lacs2.3* and *bos1 lacs2.3*. Droplets of *Botrytis* conidia suspensions (3 μl, 2×10^6 spores ml^{-1}) were applied to 24-day-old fully expanded leaves. Photographs were taken at 3 dpi. Scale bar=1 cm. (B) Quantitative lesion size data. Data of three biological repeats (n=36 in total) were analyzed in a linear mixed model with single-step P-value adjustment. Error bars represent the SE of means. Different letters above the bars indicate significant differences (P<0.05). (C) Representative wound-induced cell death symptoms stained with trypan blue. Needle-punctured leaves were stained at 6 days post wounding to detect cell death. L, Length of cell death spread; P, puncture site. Scale bar=1 mm. (D) Wound-induced cell death of *bos1* was reduced in the *bos1 lacs2.3* double mutant. Quantitative spreading cell death data. The length of spread of cell death around each wound was measured four times in four directions (up, down, left, and right), and the mean value was used. Data of three repeats were analyzed in a linear mixed model with single-step P-value adjustment. Error bars represent the SE of means. Different letters above the bars indicate significant differences (P<0.05).

the early ROS burst is not sufficient for BOS1-regulated *Botrytis* resistance.

ABA sensitivity can be uncoupled from Botrytis *immunity*

To explore the relationship between cuticle deficiency, ABA sensitivity, and *Botrytis* resistance, we analyzed the lesion sizes and cuticle permeability of multiple ABA-related mutants used in this study (Figs. 1, 2, 8) and included normalized data from our previous work (Cui *et al.*, 2016). In these mutants, a linear relationship was observed between cuticle permeability and *Botrytis* immunity (Fig. 8; R^2=0.96, P≤0.01). However, there was no correlation between ABA sensitivity and immunity. The most ABA-insensitive mutant, *112458*, which is impaired in six ABA receptors (Gonzalez-Guzman *et al.*, 2012), was more *Botrytis*-susceptible than the ABA-hypersensitive mutant *era1-2* (Fig. 8). The *lacs2.3* mutant, which was moderately impaired in ABA signaling (Wang *et al.*, 2011), was more resistant than the *snrk2.236* mutant, which is severely impaired in ABA signaling (Fig. 8). These data genetically demonstrate that *Botrytis* resistance associated with cuticle permeability could be uncoupled from ABA sensitivity.

In the *bos1* background, *Botrytis* resistance was not dependent on cuticle permeability (Fig. 8; R^2=0.52, P=0.49). Cuticle permeability in *era1-2* and *bos1 era1-2* was similar, as was the case for *lacs2.3* and *bos1 lacs2.3* (Fig. 8), indicating that BOS1 was not involved in cuticle formation. The lesion sizes of *bos1*, *bos1 era1-2*, and *bos1 lacs2.3* were proportional to the severity of their wound-induced spreading cell death phenotypes (Fig. 6C; Fig. 7C). This suggested that BOS1-regulated cell death was genetically required for cuticle-related *Botrytis* immunity.

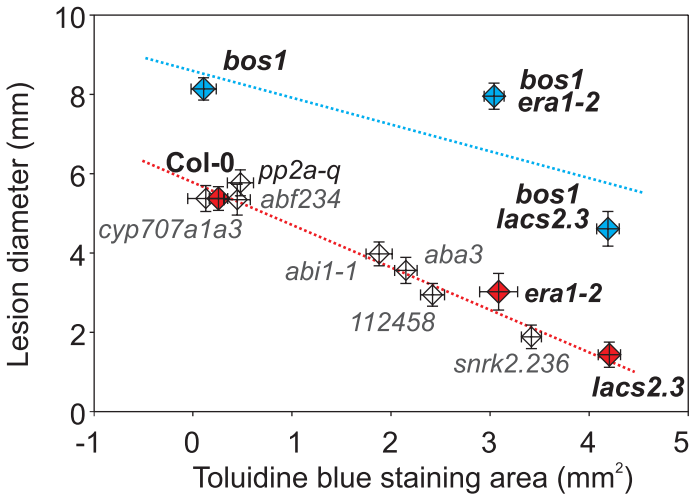

Fig. 8. ABA sensitivity is uncoupled from *Botrytis* resistance in cuticle-deficient plants. The relationship between *Botrytis* resistance and cuticle permeability of the indicated genotypes was examined. The red line was calculated with all single-mutant genotypes (not in the *bos1* background), which showed a linear correlation between cuticle permeability and lesion size (R^2=0.96, P≤0.001). The blue line was calculated with genotypes of the *bos1* background (R^2=0.52, P=0.49). The genotypes in black were examined in this study and the genotypes in grey are from previously published data (Cui *et al.*, 2016). All experiments were repeated three to six times. All the data were normalized, pooled, and analyzed with a linear model.

Role of cell-death control in enhanced Botrytis *immunity*

We previously demonstrated that impaired ABA signaling or biosynthesis could largely suppress the runaway cell-death phenotype of *bos1* (Cui *et al.*, 2013). To test the correlation between wound-induced cell death and *Botrytis* lesion size, the *aba3 bos1* and *abi1-1 bos1* double mutants were further examined with *Botrytis* droplet infection. Similar to wound-induced cell death (Cui *et al.*, 2013), *Botrytis*-induced lesions in *aba3 bos1* and *abi1-1 bos1* were significantly smaller than in *bos1* (Fig. 9A). Spray infection with *Botrytis* caused enhanced necrosis in *bos1*, which was also significantly reduced in the *aba3 bos1* and *abi1-1 bos1* double mutants (Fig. 9B). We plotted *Botrytis*-induced lesion sizes against the extent of wounding-induced cell death (Fig. 9C; this includes meta-analysis of normalized wound-induced cell death data from Cui *et al.*, 2013), and found a significant correlation (R^2=0.78, P≤0.05; Fig. 9C). Thus, the extent of cell death regulated by BOS1 plays a determinate role in the regulation of plant *Botrytis* sensitivity.

Taken together, our data illustrate that the *Botrytis* resistance in CDMs likely consists of several layered biological mechanisms. Initial resistance is conferred by pre-activated defense signaling, including increased expression of defense-related genes (Fig. 3C; Supplementary Table S2; Fig. 10). During early infection, enhanced ROS production (Fig. 1E; L'Haridon *et al.*, 2011) may augment plant defenses. At a later stage of infection, control of cell death becomes more important and determines the development of *Botrytis*-induced necrosis (Fig. 10). On the leaves of *Botrytis*-infected CDMs, cell death is dramatically attenuated at the frontier of the lesions, resulting in smaller lesion sizes compared with the wild type (Curvers *et al.*, 2010; AbuQamar *et al.*, 2017). This control of *Botrytis*-induced cell death requires BOS1 (Figs. 5–7, 10).

Discussion

Understanding the complexities of ABA signaling at the intersection between cuticle deficiency and *Botrytis* responses is challenging: ABA-deficient and -insensitive mutants are generally cuticle defective (Cui *et al.*, 2016; Martin *et al.*, 2017), while cuticle biosynthesis mutants, such as *bgd/ced1*, *lcr/cyp86a8*, *gpat4 gpat8*, and *lacs2-1*, exhibit altered stress-induced accumulation of ABA-biosynthesis transcripts and enhanced sensitivity to osmotic stress (Wang *et al.*, 2011). Here we provide new genetic data that refines the roles of pathways downstream of ABA in plant–*Botrytis* interactions.

*The role of ABA signaling in plant–*Botrytis *interactions*

Our comparisons between mutants with different levels of ABA sensitivity, cuticle permeability, and response to *Botrytis* (Fig. 8) demonstrated that cuticle permeability, but not ABA sensitivity, determines *Botrytis* resistance in CDMs. However, the role of ABA in wild-type plants is complicated during *Botrytis* infection. The application of ABA to plants results in enhanced *Botrytis* susceptibility (Audenaert *et al.*, 2002), while *Botrytis* also secretes ABA (Siewers *et al.*, 2004, 2006; Amselem *et al.*,

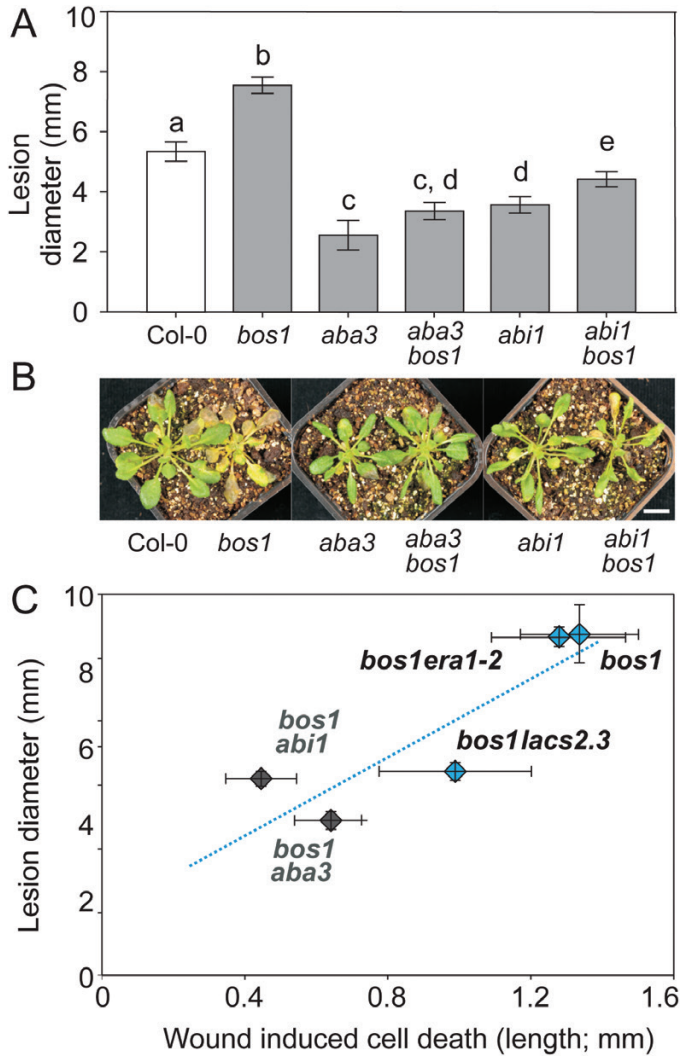

Fig. 9. *Botrytis* susceptibility of *bos1* double mutants was positively correlated with the extent of wound-induced cell death. (A) Suppressors of spreading cell death in *bos1* (*aba3-1* and *abi1-1*) also suppressed the *Botrytis* susceptibility of *bos1*. Lesion sizes from four independent experiments were combined and analyzed in a linear mixed model with a single step *P*-value adjustment. Error bars represent the SE of means (n=48 in total). Different letters above the bars indicate significant differences (P<0.05). (B) Representative symptoms of plants sprayed with *Botrytis* spore suspensions at 3 days post infection. Scale bar=1 cm. (C) *Botrytis* sensitivity correlated with the extent of wound-induced cell death in *bos1* double mutants (R^2=0.78, P=0.047). The blue dotted line shows a linear correlation between the extent of wound-induced cell death and the *Botrytis*-induced lesion sizes. The genotypes indicated with blue squares were examined in this study. The spread of cell death of the genotypes indicated with grey squares are from previously published data (Cui *et al.*, 2013), which were calculated with normalization to the reference values of the wild type and *bos1*. All experiments were repeated three to six times.

2011), which could be one mechanism used by the pathogen to promote virulence. These data would suggest ABA as a negative regulator of plant *Botrytis* immunity. In contrast, increasing ABA levels *in vivo* via drought, which doubled the ABA content in plants (Achuo *et al.*, 2006), or knocking out the ABA-degrading enzymes CYP707a1 and CYP707a3, did not alter *Botrytis* immunity (Cui *et al.*, 2016). Accordingly, the enhanced ABA sensitivities in *pp2c-q* mutants did not alter their *Botrytis* resistance either (Fig. 1A). Overexpression of the transcription factor *WRKY33* led to increased ABA sensitivity and also enhanced *Botrytis* resistance (Liu et al., 2015; Liao *et al.*, 2016). Thus, exogenous ABA is likely to have a different role from the overactivated ABA signaling *in vivo* in the course of *Botrytis* infection. ABA signaling also plays a fundamental role in several plant development processes, including determination of cell wall thickness and the number of stomata (Asselbergh *et al.*, 2007; Lake and Woodward, 2008). The long-term effects of altered ABA signaling *in vivo* (i.e. using strongly ABA-insensitive mutants) could be expected to have a stronger influence on several biological processes compared with the response to exogenous ABA application. Upon infection, ABA signaling is precisely controlled by the plant during plant–*Botrytis* interactions. A high-resolution transcriptional time-course series of *Botrytis* infection showed that repression of ABA signaling takes place at 20–22 hpi in wild type plants (Windram *et al.*, 2012). Thus, the timing and location of initiating ABA signaling should also be considered to influence the initiation or extent of cell death, to influence responses to *Botrytis* in plants.

Exogenous ABA application enhances the development of cell death symptoms (Fan *et al.*, 1997; Cui *et al.*, 2013; Takasaki *et al.*, 2015; Zhao *et al.*, 2016). The GO categories 'response to oxidative stress' and 'response to hydrogen peroxide' were enriched in the genes regulated by both ABA treatment and *Botrytis* infection at both the early and later time points (Supplementary Fig. S6). These categories are integrated in the process of cell death (Overmyer *et al.*, 2003; Van Breusegem and Dat, 2006). Thus, one role for ABA in responses to *Botrytis* could be to alter the extent of cell death. We explored this further utilizing the *bos1* mutant, which displays enhanced cell death upon ABA application and increased ROS production after both *Botrytis* infection and wounding (Mengiste *et al.*, 2003; Kraepiel *et al.*, 2011; Cui *et al.*, 2013). The *abi1-1* and *aba3* mutants suppressed the severe *Botrytis* susceptibility of *bos1*. Proportionally, these mutants also suppressed the extent of wound-induced spreading cell death in *bos1* (Fig. 9C). Thus, a linear correlation between *Botrytis* sensitivity and ABA-regulated cell death was demonstrated. This was also supported by the symptoms shown by *lacs2.3 bos1* and *era1 bos1*. The *lacs2* mutant is deficient in one step of cuticle biosynthesis, but also exhibits a secondary phenotype of deficient ABA biosynthesis (Wang *et al.*, 2011). The *lacs2.3* mutant attenuated both the runaway cell death and *Botrytis* susceptibility phenotypes of *bos1* (Fig. 7). However, *era1-2* had no effect on either of these phenotypes in *era1-2 bos1* (Fig. 6). This genetic evidence supports the hypothesis that ABA can influence *Botrytis* sensitivity through the regulation of cell death. Since ABA sensitivity had little effect in the Col-0 background (Fig. 8) but was linearly correlated with *Botrytis* susceptibility in the *bos1* background (Fig. 9C), we propose that ABA signaling could affect plant sensitivity to *Botrytis* only when it is activated at levels high enough to trigger cell death.

Resistance trade-offs in cuticle-permeable mutants

Cuticle permeability confers effective resistance to certain necrotrophic pathogens, such as *Botrytis*, but also enhances susceptibility to other pathogens (Łaźniewska *et al.*, 2012; Serrano

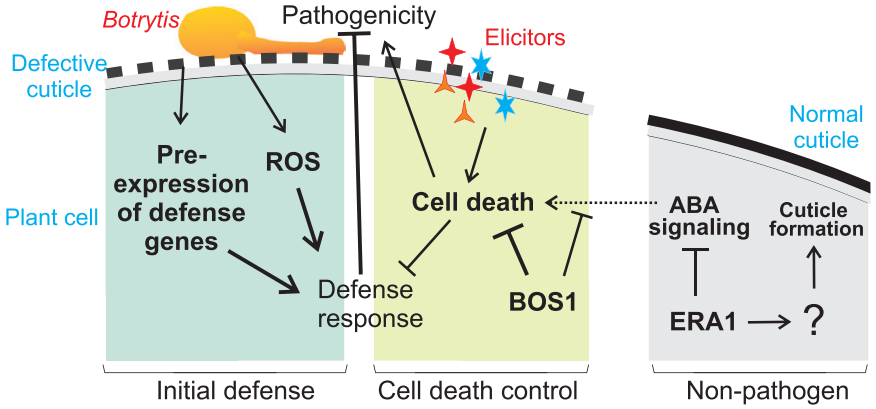

Fig. 10. Model of layered defense responses to *Botrytis* in cuticle-deficient plants. Cuticle permeability itself leads to increased expression of defense genes related to pathogen perception and salicylic acid signaling. In addition, a permeable cuticle enhances the production of reactive oxygen species (ROS), which act as signaling molecules and regulators of cell death (see also L'Haridon *et al.*, 2011). BOS1 is required to maintain cell viability and contain *Botrytis*-induced lesion expansion. The left panel represents the initial resistance and the middle panel represents a later stage of infection. The right panel illustrates signaling relationships under normal conditions, with an intact cuticle and the absence of pathogens, in which ERA1 attenuates ABA signaling and independently promotes cuticle formation via an unknown mechanism.

et al., 2014; Ziv *et al.*, 2018). This topic is attracting increasing interest, especially due to its potential use in practical breeding of economically important species (Ziv *et al.*, 2018). Our transcription data showed increased expression of many important pathogen-related genes in the CDMs even under control conditions (Supplementary Fig. S3A and S4; Supplementary Table S2A). These included genes encoding several proposed receptors that detect the presence of pathogens, such as *FLG22-induced Receptor-like Kinase 1* (*FRK1*), *Receptor Kinase 3* (*RK3*), *Cysteine-rich receptor-like protein kinase family*, and *Leucine-rich repeat protein kinase family*. Increased expression of these genes could potentially prime CDMs for responses to certain pathogens. The wounding responsive gene *Wound-Responsive 3* (*WR3*) and *NRT1/PTR Family 5.2* (*NPF5.2*) were also up-regulated. Wounding induces plant immunity to *Botrytis* (Chassot *et al.*, 2008), and pre-activation of wound-regulated signaling might facilitate the restriction of *Botrytis* pathogenicity in CDMs (Chassot *et al.*, 2008). Remarkably, the mechanism for the enhanced *Botrytis* immunity of CDMs remains unknown. The activation of defense transcripts observed here under control (*Botrytis*-free) conditions in CDMs is consistent with the proposed idea that unincorporated cuticle-building substrates that are present in CMDs may act as damage-associated molecular patterns to pre-activate immune signaling (Serrano *et al.*, 2014).

Other genes displaying higher expression in CDMs act as negative regulators in SA signaling. These included genes required for susceptibility to hemibiotrophic or biotrophic pathogens (Supplementary Table S2A, C; Supplementary Fig. S4). For example, the hemibiotrophic pathogen *P. syringae* requires *UDP-Dependent Glycosyltransferase 76B1* (*UGT76B1*; von Saint Paul *et al.*, 2011), *Lysine Histidine Transporter 1* (*LHT1*; Liu *et al.*, 2010*b*), and *WRKY DNA-Binding Protein 38* (*WRKY38*; Kim *et al.*, 2008) for pathogenicity. The biotrophic powdery mildew *Erysiphe cruciferarum* requires *Mildew Resistance Locus O12* (*MLO12*; Consonni *et al.*, 2006), *LHT1*, and *Impaired Oomycete Susceptibility 1* (*IOS1*; Hok *et al.*, 2014). The biotrophic oomycete downy mildew pathogen *H. parasitica* requires *IOS1* and *Late Upregulated in Response to Hyaloperonospora parasitica 1* (*LURP1*; Knoth and Eulgem, 2008). Finally, the hemibiotrophic species *Colletotrichum higginsianum* and *Phytophthora parasitica* require *LHT1* and *IOS1*, respectively, for pathogenicity (Consonni *et al.*, 2006; Kim *et al.*, 2008; Knoth and Eulgem, 2008; Liu *et al.*, 2010*b*; von Saint Paul *et al.*, 2011; Hok *et al.*, 2014). Differential expression of these genes might explain why cuticle-defective mutants have an altered balance between *Botrytis* resistance and biotrophic pathogen resistance, resulting in susceptibility to certain pathogens.

ERA1 in defense responses

ERA1 is the β subunit of the plant farnesyl trans-transferase, which was isolated and extensively studied for its functions related to development and abiotic stresses (Galichet and Gruissem, 2003). A few studies have also explored its role in responses to pathogens including the hemibiotrophic bacterial pathogen *P. syringae* pv. *maculicola* and the biotrophic oomycete pathogen *H. parasitica* (Goritschnig *et al.*, 2008). It was suggested that loss of function of ERA1 resulted in a mis-regulation of the interaction between ABA and defense signaling, such as SA (Goritschnig *et al.*, 2008). ERA1 adds a farnesyl to its typical substrate proteins, which contain a CaaX motif at the C-terminal (Galichet and Gruissem, 2003). ERA1 has over 700 potential targets for farnesylation; this presents a considerable challenge to identifying the relevant protein that acts as a regulator of *Botrytis* defense and/or cuticle formation (Goritschnig *et al.*, 2008; Northey *et al.*, 2016). At the same time, the existence of over 700 potential targets makes *era1* a pleiotropic mutant, as is also illustrated by its many other different phenotypes, such as aberrant flower development (Ziegelhoffer *et al.*, 2000). Thus, some caution should be taken in the interpretation of *era1* phenotypes compared with other permeability mutants. In the future, identification of the ERA1 substrate that regulates cuticle formation, for example, with a protein purification approach (Dutilleul *et al.*, 2016), could lead to the identification of the mechanisms that

regulate cuticle formation. However, even without knowledge of this ERA1 target, the robust ABA hypersensitivity and cuticle permeability of *era1* make it a useful tool to explore the interactions between ABA, cell death, cuticle permeability, and responses to *Botrytis*.

In this study, we reported the functions of ERA1 in cuticle formation and *Botrytis* resistance, genetically uncoupled plant ABA sensitivity from *Botrytis* sensitivity, and identified *bos1* as the first suppressor of *Botrytis* immunity in CDMs. These results support the hypothesis that ABA can promote susceptibility to *Botrytis* infection via the regulation of plant cell death, and provide a framework for future work on the role of ABA in the regulation of plant–*Botrytis* interactions.

Supplementary data

Supplementary data are available at *JXB* online.

Fig. S1. Increased *Botrytis* immunity in *era1-7* and *era1-8*.

Fig. S2. Cuticle permeability of known ERA1 substrates.

Fig. S3. DEGs in cuticle-defective mutants compared with Col-0 under mock and *Botrytis* treatments.

Fig. S4. Real-time quantitative reverse transcription–PCR data.

Fig. S5. Significant overlaps between ABA- and *Botrytis*-regulated genes.

Fig. S6. GO enrichment analysis of genes regulated by both ABA and *Botrytis*.

Fig. S7. Early *Botrytis*-induced ROS in *era1-2* and *lacs2.3* were not attenuated by *bos1*.

Table S1. DEGs identified in comparisons between genotypes (CDMs versus Col-0) and treatments (*Botrytis* versus mock).

Table S2. Core genes common to the DEGs of each CDM.

Table S3. *Botrytis*-responsive genes of each genotype.

Table S4. Common genes regulated by both ABA and *Botrytis*.

Table S5. Gene information and expression values used for Fig. 5.

Table S6. Primers used in this work.

Data deposition

The RNA-seq data presented in this paper have been deposited in the NCBI Sequence Read Archive (https://www.ncbi.nlm.nih.gov/sra) under accession number PRJNA495475.

Acknowledgements

We gratefully acknowledge the following for providing seeds: Dr Pedro L. Rodriguez for *pp2c-q*; Dr Xin Li for *era1-7* and *era1-8*; Dr Tesfaye Mengiste for *bos1*; and Dr Christiane Nawrath for *lacs2.3*. We gratefully acknowledge Jarkko Salojärvi (University of Helsinki) for assistance in statistical analysis; Xiaoxue Ye and Yanmei Yang for help with uploading data and exporting figures; and Tuomas Puukko, Airi Lamminmäki, and Leena Grönholm for excellent technical support. This work supported by the National Natural Science Foundation of China (grant no. 31700224 to FC and YZ, and 31871233 to WW); the Zhejiang Science and Technology Major Program on Agricultural New Variety Breeding (grant no. 2016C02056-1); the Program for Changjiang Scholars and Innovative Research Team in University (grant no. IRT_17R99 to SL); and the Academy of Finland Center of Excellence in Molecular Biology of Primary Producers 2014–2019 (Decisions no. 307335 and 271832).

References

AbuQamar S, Moustafa K, Tran LS. 2017. Mechanisms and strategies of plant defense against *Botrytis cinerea*. Critical Reviews in Biotechnology **37**, 262–274.

Achuo EA, Prinsen E, Höfte M. 2006. Influence of drought, salt stress and abscisic acid on the resistance of tomato to *Botrytis cinerea* and *Oidium neolycopersici*. Plant Pathology **55**, 178–186.

Amselem J, Cuomo CA, van Kan JA, *et al*. 2011. Genomic analysis of the necrotrophic fungal pathogens *Sclerotinia sclerotiorum* and *Botrytis cinerea*. PLoS Genetics **7**, e1002230.

Antoni R, Gonzalez-Guzman M, Rodriguez L, *et al*. 2013. PYRABACTIN RESISTANCE1-LIKE8 plays an important role for the regulation of abscisic acid signaling in root. Plant Physiology **161**, 931–941.

Asselbergh B, Curvers K, Franca SC, Audenaert K, Vuylsteke M, Van Breusegem F, Höfte M. 2007. Resistance to *Botrytis cinerea* in *sitiens*, an abscisic acid-deficient tomato mutant, involves timely production of hydrogen peroxide and cell wall modifications in the epidermis. Plant Physiology **144**, 1863–1877.

Audenaert K, De Meyer GB, Höfte MM. 2002. Abscisic acid determines basal susceptibility of tomato to *Botrytis cinerea* and suppresses salicylic acid-dependent signaling mechanisms. Plant Physiology **128**, 491–501.

Bessire M, Chassot C, Jacquat AC, Humphry M, Borel S, Petétot JM, Métraux JP, Nawrath C. 2007. A permeable cuticle in *Arabidopsis* leads to a strong resistance to *Botrytis cinerea*. The EMBO Journal **26**, 2158–2168.

Bolger AM, Lohse M, Usadel B. 2014. Trimmomatic: a flexible trimmer for Illumina sequence data. Bioinformatics **30**, 2114–2120.

Chassot C, Buchala A, Schoonbeek HJ, Métraux JP, Lamotte O. 2008. Wounding of Arabidopsis leaves causes a powerful but transient protection against *Botrytis* infection. The Plant Journal **55**, 555–567.

Chassot C, Nawrath C, Métraux JP. 2007. Cuticular defects lead to full immunity to a major plant pathogen. The Plant Journal **49**, 972–980.

Consonni C, Humphry ME, Hartmann HA, *et al*. 2006. Conserved requirement for a plant host cell protein in powdery mildew pathogenesis. Nature Genetics **38**, 716–720.

Cui F, Brosché M, Lehtonen MT, Amiryousefi A, Xu E, Punkkinen M, Valkonen JP, Fujii H, Overmyer K. 2016. Dissecting abscisic acid signaling pathways involved in cuticle formation. Molecular Plant **9**, 926–938.

Cui F, Brosché M, Sipari N, Tang S, Overmyer K. 2013. Regulation of ABA dependent wound induced spreading cell death by MYB108. New Phytologist **200**, 634–640.

Curvers K, Seifi H, Mouille G, *et al*. 2010. Abscisic acid deficiency causes changes in cuticle permeability and pectin composition that influence tomato resistance to *Botrytis cinerea*. Plant Physiology **154**, 847–860.

Cutler S, Ghassemian M, Bonetta D, Cooney S, McCourt P. 1996. A protein farnesyl transferase involved in abscisic acid signal transduction in *Arabidopsis*. Science **273**, 1239–1241.

Dean R, Van Kan JA, Pretorius ZA, *et al*. 2012. The Top 10 fungal pathogens in molecular plant pathology. Molecular Plant Pathology **13**, 414–430.

Dutilleul C, Ribeiro I, Blanc N, *et al*. 2016. ASG2 is a farnesylated DWD protein that acts as ABA negative regulator in *Arabidopsis*. Plant, Cell & Environment **39**, 185–198.

Fan L, Zheng S, Wang X. 1997. Antisense suppression of phospholipase D alpha retards abscisic acid- and ethylene-promoted senescence of postharvest Arabidopsis leaves. The Plant Cell **9**, 2183–2196.

Fujii H, Zhu J-K. 2009. Arabidopsis mutant deficient in 3 abscisic acid-activated protein kinases reveals critical roles in growth, reproduction, and stress. Proceedings of the National Academy of Sciences, USA **106**, 8380–8385.

Gachon C, Saindrenan P. 2004. Real-time PCR monitoring of fungal development in *Arabidopsis thaliana* infected by *Alternaria brassicicola* and *Botrytis cinerea*. Plant Physiology and Biochemistry **42**, 367–371.

Galichet A, Gruissem W. 2003. Protein farnesylation in plants–conserved mechanisms but different targets. Current Opinion in Plant Biology **6**, 530–535.

Galichet A, Gruissem W. 2006. Developmentally controlled farnesylation modulates AtNAP1;1 function in cell proliferation and cell expansion during Arabidopsis leaf development. Plant Physiology **142**, 1412–1426.

Gonzalez-Guzman M, Pizzio GA, Antoni R, *et al.* 2012. *Arabidopsis* PYR/PYL/RCAR receptors play a major role in quantitative regulation of stomatal aperture and transcriptional response to abscisic acid. The Plant Cell **24**, 2483–2496.

Goritschnig S, Weihmann T, Zhang Y, Fobert P, McCourt P, Li X. 2008. A novel role for protein farnesylation in plant innate immunity. Plant Physiology **148**, 348–357.

Hellemans J, Mortier G, De Paepe A, Speleman F, Vandesompele J. 2007. qBase relative quantification framework and software for management and automated analysis of real-time quantitative PCR data. Genome Biology **8**, R19.

Hok S, Allasia V, Andrio E, *et al.* 2014. The receptor kinase IMPAIRED OOMYCETE SUSCEPTIBILITY1 attenuates abscisic acid responses in Arabidopsis. Plant Physiology **166**, 1506–1518.

Jiang M, Zhang J. 2001. Effect of abscisic acid on active oxygen species, antioxidative defence system and oxidative damage in leaves of maize seedlings. Plant & Cell Physiology **42**, 1265–1273.

Jalakas P, Huang YC, Yeh YH, Zimmerli L, Merilo E, Kollist H, Brosché M. 2017. The role of ENHANCED RESPONSES TO ABA1 (ERA1) in Arabidopsis stomatal responses is beyond ABA signaling. Plant Physiology **174**, 665–671.

Kettner J, Dörffling K. 1995. Biosynthesis and metabolism of abscisic acid in tomato leaves infected with *Botrytis cinerea*. Planta **196**, 627–634.

Kim KC, Lai Z, Fan B, Chen Z. 2008. *Arabidopsis* WRKY38 and WRKY62 transcription factors interact with histone deacetylase 19 in basal defense. The Plant Cell **20**, 2357–2371.

Kim D, Langmead B, Salzberg SL. 2015. HISAT: a fast spliced aligner with low memory requirements. Nature Methods **12**, 357–360.

Kliebenstein DJ, Rowe HC, Denby KJ. 2005. Secondary metabolites influence *Arabidopsis*/*Botrytis* interactions: variation in host production and pathogen sensitivity. The Plant Journal **44**, 25–36.

Knoth C, Eulgem T. 2008. The oomycete response gene *LURP1* is required for defense against *Hyaloperonospora parasitica* in *Arabidopsis thaliana*. The Plant Journal **55**, 53–64.

Kraepiel Y, Pédron J, Patrit O, Simond-Côte E, Hermand V, Van Gijsegem F. 2011. Analysis of the plant *bos1* mutant highlights necrosis as an efficient defence mechanism during *D. dadantii*/*Arabidospis thaliana* interaction. PLoS One **6**, e18991.

Łaźniewska J, Macioszek VK, Kononowicz AK. 2012. Plant-fungus interface: the role of surface structures in plant resistance and susceptibility to pathogenic fungi. Physiological and Molecular Plant Pathology **78**, 24–30.

L'Haridon F, Besson-Bard A, Binda M, *et al.* 2011. A permeable cuticle is associated with the release of reactive oxygen species and induction of innate immunity. PLoS Pathogens **7**, e1002148.

Lake JA, Woodward FI. 2008. Response of stomatal numbers to CO_2 and humidity: control by transpiration rate and abscisic acid. New Phytologist **179**, 397–404.

Li Y, Kabbage M, Liu W, Dickman MB. 2016. Aspartyl protease-mediated cleavage of BAG6 is necessary for autophagy and fungal resistance in plants. The Plant Cell **28**, 233–247.

Liao CJ, Lai Z, Lee S, Yun DJ, Mengiste T. 2016. Arabidopsis HOOKLESS1 regulates responses to pathogens and abscisic acid through interaction with MED18 and acetylation of *WRKY33* and *ABI5* chromatin. The Plant Cell **28**, 1662–1681.

Lionetti V, Fabri E, De Caroli M, Hansen AR, Willats WG, Piro G, Bellincampi D. 2017. Three pectin methylesterase inhibitors protect cell wall integrity for Arabidopsis immunity to *Botrytis*. Plant Physiology **173**, 1844–1863.

Liu F, Jiang H, Ye S, *et al.* 2010c. The *Arabidopsis* P450 protein CYP82C2 modulates jasmonate-induced root growth inhibition, defense gene expression and indole glucosinolate biosynthesis. Cell Research **20**, 539–552.

Liu G, Ji Y, Bhuiyan NH, Pilot G, Selvaraj G, Zou J, Wei Y. 2010b. Amino acid homeostasis modulates salicylic acid-associated redox status and defense responses in *Arabidopsis*. The Plant Cell **22**, 3845–3863.

Liu S, Kracher B, Ziegler J, Birkenbihl RP, Somssich IE. 2015. Negative regulation of ABA signaling by WRKY33 is critical for *Arabidopsis* immunity towards *Botrytis cinerea* 2100. eLife **4**, e07295.

Liu Y, He J, Chen Z, Ren X, Hong X, Gong Z. 2010a. ABA *overly-sensitive 5* (*ABO5*), encoding a pentatricopeptide repeat protein required for *cis*-splicing of mitochondrial *nad2* intron 3, is involved in the abscisic acid response in Arabidopsis. The Plant Journal **63**, 749–765.

Love MI, Huber W, Anders S. 2014. Moderated estimation of fold change and dispersion for RNA-seq data with DESeq2. Genome Biology **15**, 550.

Martin LBB, Romero P, Fich EA, Domozych DS, Rose JKC. 2017. Cuticle biosynthesis in tomato leaves is developmentally regulated by abscisic acid. Plant Physiology **174**, 1384–1398.

Mengiste T. 2012. Plant immunity to necrotrophs. Annual Review of Phytopathology **50**, 267–294.

Mengiste T, Chen X, Salmeron J, Dietrich R. 2003. The *BOTRYTIS SUSCEPTIBLE1* gene encodes an R2R3MYB transcription factor protein that is required for biotic and abiotic stress responses in Arabidopsis. The Plant Cell **15**, 2551–2565.

Northey JG, Liang S, Jamshed M, Deb S, Foo E, Reid JB, McCourt P, Samuel MA. 2016. Farnesylation mediates brassinosteroid biosynthesis to regulate abscisic acid responses. Nature Plants **2**, 16114.

O'Brien TP, Feder N, McCully ME. 1964. Polychromatic staining of plant cell walls by toluidine blue O. Protoplasma **59**, 368–373.

Okamoto M, Kuwahara A, Seo M, Kushiro T, Asami T, Hirai N, Kamiya Y, Koshiba T, Nambara E. 2006. CYP707A1 and CYP707A2, which encode abscisic acid 8′-hydroxylases, are indispensable for proper control of seed dormancy and germination in Arabidopsis. Plant Physiology **141**, 97–107.

Overmyer K, Brosché M, Kangasjärvi J. 2003. Reactive oxygen species and hormonal control of cell death. Trends in Plant Science **8**, 335–342.

Park SY, Fung P, Nishimura N, *et al.* 2009. Abscisic acid inhibits type 2C protein phosphatases via the PYR/PYL family of START proteins. Science **324**, 1068–1071.

Pei ZM, Ghassemian M, Kwak CM, McCourt P, Schroeder JI. 1998. Role of farnesyltransferase in ABA regulation of guard cell anion channels and plant water loss. Science **282**, 287–290.

Pertea M, Pertea GM, Antonescu CM, Chang TC, Mendell JT, Salzberg SL. 2015. StringTie enables improved reconstruction of a transcriptome from RNA-seq reads. Nature Biotechnology **33**, 290–295.

Rajniak J, Barco B, Clay NK, Sattely ES. 2015. A new cyanogenic metabolite in *Arabidopsis* required for inducible pathogen defence. Nature **525**, 376–379.

Riederer M. 2007. Introduction: biology of the plant cuticle. In: Riederer M, Müller C, eds. Annual Plant Reviews. Volume 23: Biology of the plant cuticle. Oxford: Blackwell, 1–10.

Ritpitakphong U, Falquet L, Vimoltust A, Berger A, Métraux JP, L'Haridon F. 2016. The microbiome of the leaf surface of Arabidopsis protects against a fungal pathogen. New Phytologist **210**, 1033–1043.

Robinson MD, McCarthy DJ, Smyth GK. 2010. edgeR: a Bioconductor package for differential expression analysis of digital gene expression data. Bioinformatics **26**, 139–140.

Rubio S, Rodrigues A, Saez A, Dizon MB, Galle A, Kim TH, Santiago J, Flexas J, Schroeder JI, Rodriguez PL. 2009. Triple loss of function of protein phosphatases type 2C leads to partial constitutive response to endogenous abscisic acid. Plant Physiology **150**, 1345–1355.

Seifi HS, Curvers K, De Vleesschauwer D, Delaere I, Aziz A, Höfte M. 2013. Concurrent overactivation of the cytosolic glutamine synthetase and the GABA shunt in the ABA-deficient *sitiens* mutant of tomato leads to resistance against *Botrytis cinerea*. New Phytologist **199**, 490–504.

Serrano M, Coluccia F, Torres M, L'Haridon F, Métraux JP. 2014. The cuticle and plant defense to pathogens. Frontiers in Plant Science **5**, 274.

Shaul O, Elad Y, Zieslin N. 1996. Suppression of *Botrytis* blight in cut rose flowers with gibberellic acid. Effects of exogenous application of abscisic acid and paclobutrazol. Postharvest Biology and Technology **7**, 145–150.

Siewers V, Kokkelink L, Smedsgaard J, Tudzynski P. 2006. Identification of an abscisic acid gene cluster in the grey mold *Botrytis cinerea*. Applied and Environmental Microbiology **72**, 4619–4626.

Siewers V, Smedsgaard J, Tudzynski P. 2004. The P450 monooxygenase BcABA1 is essential for abscisic acid biosynthesis in *Botrytis cinerea*. Applied and Environmental Microbiology **70**, 3868–3876.

Takasaki H, Maruyama K, Takahashi F, Fujita M, Yoshida T, Nakashima K, Myouga F, Toyooka K, Yamaguchi-Shinozaki K, Shinozaki K. 2015. SNAC-As, stress-responsive NAC transcription factors, mediate ABA-inducible leaf senescence. The Plant Journal **84**, 1114–1123.

Tanaka T, Tanaka H, Machida C, Watanabe M, Machida Y. 2004. A new method for rapid visualization of defects in leaf cuticle reveals five intrinsic patterns of surface defects in *Arabidopsis*. The Plant Journal **37**, 139–146.

Tang D, Simonich MT, Innes RW. 2007. Mutations in *LACS2*, a long-chain acyl-coenzyme A synthetase, enhance susceptibility to avirulent *Pseudomonas syringae* but confer resistance to *Botrytis cinerea* in Arabidopsis. Plant Physiology **144**, 1093–1103.

Trapnell C, Hendrickson DG, Sauvageau M, Goff L, Rinn JL, Pachter L. 2013. Differential analysis of gene regulation at transcript resolution with RNA-seq. Nature Biotechnology **31**, 46–53.

Van Breusegem F, Dat JF. 2006. Reactive oxygen species in plant cell death. Plant Physiology **141**, 384–390.

van Damme M, Huibers RP, Elberse J, Van den Ackerveken G. 2008. Arabidopsis *DMR6* encodes a putative 2OG-Fe(II) oxygenase that is defense-associated but required for susceptibility to downy mildew. The Plant Journal **54**, 785–793.

von Saint Paul V, Zhang W, Kanawati B, Geist B, Faus-Kessler T, Schmitt-Kopplin P, Schäffner AR. 2011. The *Arabidopsis* glucosyltransferase UGT76B1 conjugates isoleucic acid and modulates plant defense and senescence. The Plant Cell **23**, 4124–4145.

Wang ZY, Xiong L, Li W, Zhu JK, Zhu J. 2011. The plant cuticle is required for osmotic stress regulation of abscisic acid biosynthesis and osmotic stress tolerance in *Arabidopsis*. The Plant Cell **23**, 1971–1984.

Windram O, Madhou P, McHattie S, *et al.* 2012. *Arabidopsis* defense against *Botrytis cinerea*: chronology and regulation deciphered by high-resolution temporal transcriptomic analysis. The Plant Cell **24**, 3530–3557.

Wu G, Liu S, Zhao Y, Wang W, Kong Z, Tang D. 2015. ENHANCED DISEASE RESISTANCE4 associates with CLATHRIN HEAVY CHAIN2 and modulates plant immunity by regulating relocation of EDR1 in Arabidopsis. The Plant Cell **27**, 857–873.

Zhao Y, Chan Z, Gao J, *et al*. 2016. ABA receptor PYL9 promotes drought resistance and leaf senescence. Proceedings of the National Academy of Sciences **113**, 1949–1954.

Zhu Y, Wang B, Tang K, Hsu CC, Xie S, Du H, Yang Y, Tao WA, Zhu JK. 2017. An *Arabidopsis* Nucleoporin *NUP85* modulates plant responses to ABA and salt stress. PLoS Genetics **13**, e1007124.

Ziegelhoffer EC, Medrano LJ, Meyerowitz EM. 2000. Cloning of the *Arabidopsis WIGGUM* gene identifies a role for farnesylation in meristem development. Proceedings of the National Academy of Sciences, USA **97**, 7633–7638.

Ziv C, Zhao Z, Gao YG, Xia Y. 2018. Multifunctional roles of plant cuticle during plant-pathogen interactions. Frontiers in Plant Science **9**, 1088.